*electronics*

MDPI

*Article*

# A Novel Multifunctional Negative Group Delay Circuit for Realizing Band-Pass, High-Pass and Low-Pass

**Aixia Yuan [1,2], Shaojun Fang [1,*], Zhongbao Wang [1] and Hongmei Liu [1]**

[1] School of Information Science and Technology, Dalian Maritime University, Dalian 116026, China; yuanax@dlpu.edu.cn (A.Y.); wangzb@dlmu.edu.cn (Z.W.); lhm323@dlmu.edu.cn (H.L.)
[2] School of Information Science and Engineering, Dalian Polytechnic University, Dalian 116034, China
* Correspondence: fangshj@dlmu.edu.cn

**Abstract:** A novel multifunctional negative group delay circuit is proposed. The circuit can realize three different negative group delay functions, including band-pass, high-pass and low-pass, which meet different conditions with capacitance, inductance and resistance. Analytical design equations are provided. The effects of different element values on the bandwidth, cut-off frequency and the minimum negative group delay of the circuit are analyzed. According to this design method, the negative group delay circuit is designed and fabricated. Simulation and measurement results are in agreement. It has good negative group delay characteristics. The feasibility of the design method is verified.

**Keywords:** negative group delay; band-pass; high-pass; low-pass



**Citation:** Yuan, A.; Fang, S.; Wang, Z.; Liu, H. A Novel Multifunctional Negative Group Delay Circuit for Realizing Band-Pass, High-Pass and Low-Pass. *Electronics* **2021**, *10*, 1742. https://doi.org/10.3390/electronics10141742

Academic Editor: Fabian Khateb

Received: 21 June 2021
Accepted: 16 July 2021
Published: 20 July 2021



## 1. Introduction

Low latency is an important goal of modern communications. The group delay effect reduces the performance of the electronic circuit, limits the operating speed of the electronic system [1,2] and affects the performance of the communication system [3,4]. In order to eliminate the influence of group delay, many studies have been carried out. A group delay compensation technology is proposed in [5–8]. The synchronization technology based on memristive elements to maintain the integrity of the signal waveform is implemented in [9,10], but this technology will increase the power consumption of the system. A method to reduce the group delay based on the all-pass network is designed in [11,12]. This method can reduce the dispersion effect, but the reduction in the group delay is not obvious.

Negative group delay (NGD) technology has attracted attention for reducing the influence of group delay. Since the phenomenon of negative group delay is confirmed by experiments, scholars have carried out a lot of research work on negative group delay [13–29]. An equalization technique based on negative group delay is proposed in [13,14], which can reconstruct the signals changed by time delay. Negative group delay technology can be used in antenna design to improve the performance of array antennas [15,16]. A power divider with negative group delay characteristics is designed in [17]. An original circuit theory that can identify and synthesize simple band-pass negative group delay (NGD) circuit topologies is presented in [18]. A first-order low-pass negative group delay topology is proposed in [19]. The synthesis and design of high-pass NGD network impedance is given in [20]. The passive NGD circuit using an RLC resonant circuit is studied in [26]. The resonator works at different resonant frequencies to realize the broadband NGD circuit. A novel design for a dual-band negative group delay circuit (NGDC) is proposed in [27]. A full-passband linear-phase band-pass filter (BPF) equalized with negative group delay circuits (NGDC) is proposed in [28]. An absorptive bandstop filter is proposed and synthesized with prescribed negative group delay (NGD) and negative group delay bandwidth (NBW) in [29].

The existing negative group delay circuits all use one circuit to achieve a single function. This article proposes a novel multifunctional negative group delay circuit, which implements three negative group delay functions. If the element values are in different ranges, there will be three different negative group delay circuits of band-pass, high-pass and low-pass. This circuit has good negative group delay performance and insertion loss. For the negative group delay of band-pass, high-pass and low-pass circuits, the influence of element values on the center frequency, cut-off frequency and minimum negative group delay of the negative group delay circuit is given.

This paper consists of three main parts. The second section introduces the structure of this circuit. Through equation derivation, the conditions for the band-pass, high-pass and low-pass negative group delay characteristics of the circuit are demonstrated. The third section discusses the relationship between the minimum negative group delay and the element value of the negative group delay circuit. In the fourth section, the theory, simulation and measurement are carried out. The calculation and circuit simulation are given. The final part of the paper is the conclusion.

## 2. Multifunctional Negative Group Delay Circuit

A novel multifunctional negative group delay circuit is proposed. As shown in Figure 1, this circuit can realize band-pass, high-pass and low-pass negative group delays when the capacitor, inductor and resistor take different values.

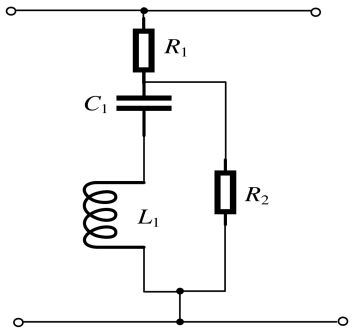


**Figure 1.** Negative group delay circuit.

### *2.1. Band-Pass and High-Pass Negative Group Delay Circuits Analysis*

The impedance of the negative group delay circuit is Equation (1). The characteristic impedance of the circuit is $Z_0$. The transfer function of the circuit is Equation (2), and the group delay is Equation (3).

$$Z = R_1 + \frac{R_2(\frac{1}{j\omega C_1} + j\omega L_1)}{R_2 + \frac{1}{j\omega C_1} + j\omega L_1} \tag{1}$$

$$S_{21} = \frac{2Z_0}{2Z_0 + Z_0^2/Z} = \frac{2(R_1 + R_2 - C_1L_1R_1\omega^2 - C_1L_1R_2\omega^2 + jC_1R_1R_2\omega)}{2R_1 + 2R_2 + Z_0 - 2C_1L_1R_1\omega^2 - 2C_1L_1R_2\omega^2 - C_1L_1Z_0\omega^2 + 2jC_1R_1R_2\omega + jC_1R_2Z_0\omega} \tag{2}$$

$$\tau(\omega) = -\frac{\partial \angle S_{21}}{\partial \omega} \tag{3}$$

According to Equation (3), when $\omega = 0$, $C_1$, $R_1$, $R_2$ and $Z_0$ satisfy the Equation (4). $\tau$ denotes the group delay value at $\omega = 0$. At this time, $\tau$ is independent of $L_1$. The magnitude of $\tau$ is used as one of the bases to distinguish the delay types of negative groups.

$$\tau_{(\omega=0)} = \frac{C_1 R_2^2 Z_0^3 (2R_1^2 + 4R_1R_2 + Z_0R_1 + 2R_2^2 + Z_0R_2)^3}{\left(\frac{2Z_0+Z_0^2}{R_1+R_2}\right)^2 (R_1^2 + 2R_1R_2 + R_2^2)^3 (4R_1^2 + 8R_1R_2 + 4R_1Z_0 + 4R_2^2 + 4R_2Z_0 + Z_0^2)} \tag{4}$$

When $\tau = 0$, $R_1 = R_2 = Z_0 = 50\ \Omega$, according to Equation (3); two significant frequency values are calculated, which are respectively Equations (5) and (6). The bandwidth of the negative group delay circuit is shown in Equation (7). $f_0$ represents the frequency corresponding to the minimum value of negative group delay in Equation (8), when the circuit presents band-pass characteristics.

$$f_2 = \frac{\sqrt{375C_1^2 + 5\sqrt{15}\sqrt{C_1^3(375C_1 + 2L_1)} + C_1L_1}}{2\pi C_1 L_1} \tag{5}$$

$$f_1 = \frac{\sqrt{375C_1^2 - 5\sqrt{15}\sqrt{C_1^3(375C_1 + 2L_1)} + C_1L_1}}{2\pi C_1 L_1} \tag{6}$$

$$\mathrm{BW_{NGD}} = f_2 - f_1 \tag{7}$$

$$f_0 = \sqrt{f_1 f_2} \tag{8}$$

The circuit shown in Figure 1 is a band-pass negative group delay circuit if Equation (9) is satisfied. It is a high-pass negative group delay circuit if Equation (10) is satisfied.

$$\begin{cases} \tau > 0 (f \approx 0) \\ f_2 - f_0 \approx f_0 - f_1 \end{cases} \tag{9}$$

$$\begin{cases} \tau \geq 0 (f \approx 0) \\ f_2 - f_0 \gg f_0 - f_1 \end{cases} \tag{10}$$

*2.2. Low-Pass Negative Group Delay Circuit Analysis*

If there is no capacitor in Figure 1, the impedance of the circuit is shown in Equation (11). The transmission function is shown in Equation (12). A low-pass negative group delay circuit will be obtained.

$$Z = R_1 + \frac{R_2(j\omega L_1)}{R_2 + j\omega L_1} \tag{11}$$

$$S_{21} = \frac{2(L_1R_1\omega - jR_1R_2 + L_1R_2\omega)}{2L_1R_1\omega + 2L_1R_2\omega - jR_2Z_0 - 2jR_1R_2 + L_1Z_0\omega} \tag{12}$$

According to Equation (3), when $f = 0$, the NGD value and $L_1$ satisfy the relationship (13). The NGD depends on the value of the inductance in the circuit. The larger the inductance, the smaller the negative group delay.

$$f = 0,\ \tau = -\frac{1}{150}L_1 \tag{13}$$

The cut-off frequency $f_c$ of the low-pass NGD circuit is obtained when the group delay $\tau = 0$. According to Equations (12) and (3), a practical frequency value is calculated as $f_c$, and the expression such as (14). When the resistance and characteristic impedance are both fixed values, the cut-off frequency decreases as the inductance increases. When Equation (15) is satisfied, the circuit is a low-pass negative group delay circuit.

$$f_c = \frac{R_2\sqrt{R_1(R_1 + R_2)(2R_1 + Z_0)(2R_1 + 2R_2 + Z_0)}}{2\pi L_1(2R_1^2 + 4R_1R_2 + R_1Z_0 + 2R_2^2 + R_2Z_0)} (\tau = 0) \tag{14}$$

$$\begin{cases} \tau < 0 (f = 0) \\ \text{There is only one real solution.} \end{cases} \tag{15}$$

## 3. Simulation and Discussion of NGD Circuit with Different Element Values

The minimum NGD, insertion loss, center frequency, cut-off frequency and other parameters of the NGD circuit will all be affected by the element value, which will be discussed separately below.

### *3.1. Analyze the Band-Pass NGD Circuit*

#### 3.1.1. Influence of $L_1$ and $C_1$ on Band-Pass NGD

The negative group delay $\tau$ and inductance $L_1$ satisfy Equation (16) when the capacitance and resistance remain unchanged. Capacitance $C_1$ = 1.6 pF, resistance $R_1 = R_2 = Z_0$ = 50 Ω. When the inductance increases, the negative group delay $\tau$ becomes smaller.

$$\tau = \frac{1.9 \times 10^{41} L_1 \times (5.5 \times 10^{18} L_1 - 7.2 \times 10^{42})}{6.1 \times 10^{37} L_1^2 + 1.6 \times 10^{62} L_1 + 1.03 \times 10^{86}} \approx -13.7 \times 10^{-3} L_1 \tag{16}$$

When the capacitance and resistance are constant, the NGD bandwidth and center frequency decrease with the decrease of inductance. The simulation results are shown in Figure 2 and Table 1. The frequency range selected during simulation can be used for TV and data broadcasting.

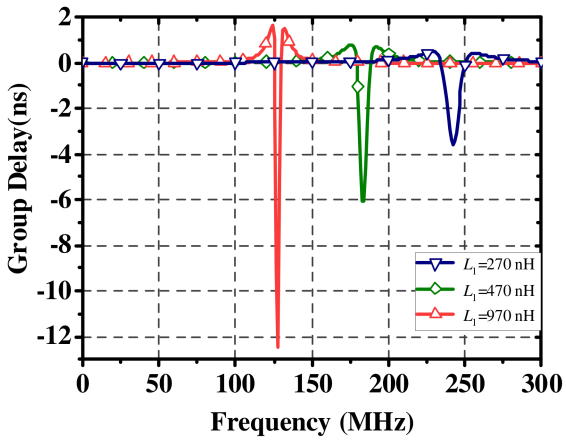


**Figure 2.** Group delay of band-pass negative group delay circuit with different inductance $L_1$.

**Table 1.** Data of band-pass negative group delay circuit with different inductance.

| State | $C_1$ (pF) | $L_1$ (nH) | $R_1$, $R_2$ (Ω) | $f_0$ (MHz) | $\tau(f_0)$ (ns) | IL (dB) |
|---|---|---|---|---|---|---|
| State1 | 1.6 | 270 | 50 | 242 | −3.59 | 3.5 |
| State2 | 1.6 | 470 | 50 | 184 | −6.06 | 3.5 |
| State3 | 1.6 | 970 | 50 | 128 | −12.45 | 3.5 |

$f_0$ refers to the frequency with the minimum negative group delay. $\tau(f_0)$ corresponds to the minimum negative group delay at frequency $f_0$. IL is insertion loss at $f_0$.

According to Equation (3), inductance $L_1$ = 470 nH, and resistance $R_1 = R_2 = Z_0$ = 50 Ω are substituted into Equation (3). Equation (17) is obtained. The capacitance $C_1$ has almost no effect on the negative group delay, but the center frequency $f_0$ of the minimum negative group delay varies with the capacitance $C_1$. When the capacitance $C_1$ is changed, and the inductance $L_1$ = 470 nH, the resistance $R_1 = R_2 = Z_0$ = 50 Ω, and the negative group delay remains $\tau \approx -6.26$ ns.

$$\tau = -\frac{3 \times 10^{43} C_1 \times (4.8 \times 10^{51} C_1 - 3.8 \times 10^{10})}{2.3 \times 10^{103} C_1^2 + 3.7 \times 10^{62} C_1 + 1.45 \times 10^{21}} = -\frac{14.4 C_1^2 - 11.4 \times 10^{-41} C_1}{2.3 \times 10^{9} C_1^2 + 3.7 \times 10^{-32} C_1 + 1.45 \times 10^{-73}} \approx -6.26 \text{ ns} \tag{17}$$

3.1.2. Influence of $R_1$ on Band-Pass NGD

On the basis of Equations (2) and (3), the resistance $R_2$, the inductance $L_1$, and the capacitor $C_1$ remain unchanged, and the resistance $R_1$ is changed. The smaller the resistance $R_1$, the smaller the negative group delay value. Negative group delay $\tau(f_0) \approx -146$ ns when $R_1 = 5\ \Omega$, and it is $\tau(f_0) \approx -250$ ns when $R_1 = 0.5\ \Omega$. The simulation results are shown in Figure 3, and the performance data are shown in Table 2. The frequency of about 21 MHz can be used for long-distance short-wave communication.

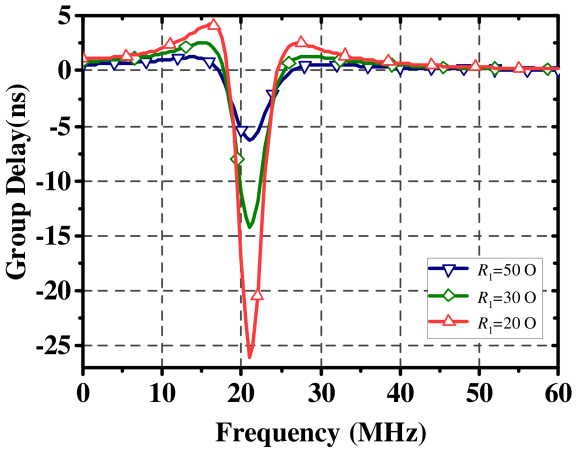


**Figure 3.** Band-pass negative group delay with different $R_1$.

**Table 2.** Data of band-pass negative group delay circuit with different $R_1$.

| State | $C_1$ (pF) | $L_1$ (nH) | $R_1$ (Ω) | $R_2$ (Ω) | $f_0$ (MHz) | $\tau(f_0)$ (ns) | IL (dB) |
|---|---|---|---|---|---|---|---|
| State1 | 120 | 470 | 50 | 50 | 21 | −6.29 | 3.5 |
| State2 | 120 | 470 | 30 | 50 | 21 | −14.26 | 5.2 |
| State3 | 120 | 470 | 20 | 50 | 21 | −26.03 | 7.0 |

3.1.3. Influence of $R_2$ on Band-Pass NGD

The resistance $R_2$ mainly affects the bandwidth of negative group delay circuits. When changing the resistance $R_2$, the resistance $R_1$, the inductance $L_1$ and the capacitance $C_1$ remain unchanged. When the resistance value $R_2$ increases, the bandwidth of the negative group delay circuit increases. The negative group delay basically remains unchanged when $R_2$ is greater than 50 Ω. The insertion loss at $f_0$ is about 3.5 dB which basically remains unchanged. The simulation results are shown in Figure 4, and the performance data are shown in Table 3.

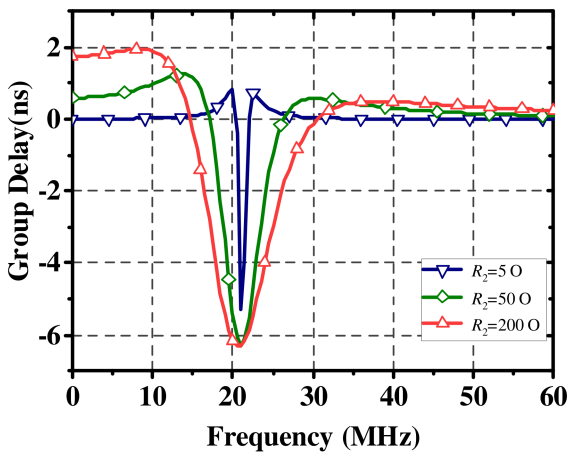


**Figure 4.** Band-pass negative group delay with different $R_2$.

**Table 3.** Data of band-pass negative group delay circuit with different $R_2$.

| State | $C_1$ (pF) | $L_1$ (nH) | $R_1$ (Ω) | $R_2$ (Ω) | $f_0$ (MHz) | $\tau(f_0)$ (ns) | NGD Band (MHz) |
|---|---|---|---|---|---|---|---|
| State1 | 120 | 470 | 50 | 5 | 21 | −5.28 | 1.56 |
| State2 | 120 | 470 | 50 | 50 | 21 | −6.29 | 9.28 |
| State3 | 120 | 470 | 50 | 200 | 21 | −6.32 | 15.83 |

### 3.2. High-Pass NGD Circuit

According to the values of $L_1$, $C_1$, $R_1$ and $R_2$ in Table 4, the circuit presents a high-pass negative group delay circuit. The negative group delay decreases with the increase of capacitance, while the inductance and resistance remain unchanged. The simulation results are shown in Figure 5. The frequency range of 461–671 kHz is suitable for marine communication and medium range navigation.

**Table 4.** Data of high-pass negative group delay circuit with different $C_1$.

| State | $C_1$ (nF) | $L_1$ (nH) | $R_1$ (Ω) | $R_2$ (Ω) | $f_{opt}$ (kHz) | $\tau(f_{opt})$ (ns) | IL (dB) |
|---|---|---|---|---|---|---|---|
| State1 | 15 | 3.9 | 50 | 50 | 671 | −9.35 | 3.1 |
| State2 | 18 | 3.9 | 50 | 50 | 561 | −11.21 | 3.1 |
| State3 | 22 | 3.9 | 50 | 50 | 461 | −13.69 | 3.1 |

$f_{opt}$ refers to the frequency with the minimum negative group delay. $\tau(f_{opt})$ corresponds to the minimum negative group delay at frequency $f_{opt}$, and IL refers to the insertion loss at $f_{opt}$ frequency.

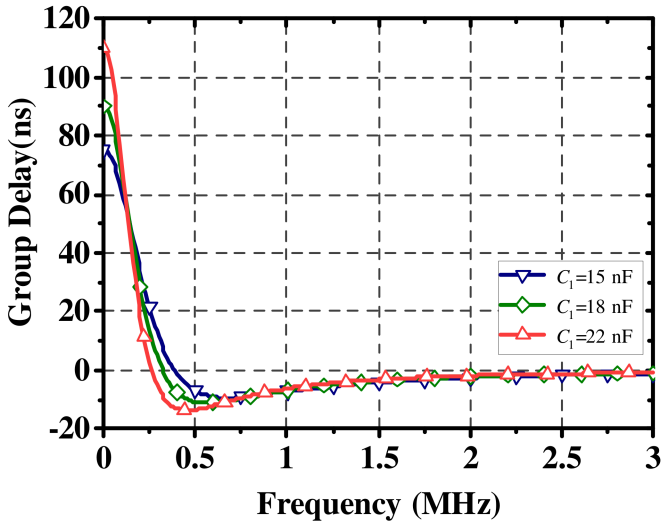


**Figure 5.** High-pass negative group delay with different capacitance.

### 3.3. Low-Pass NGD Circuit

The circuit appears as a low-pass NGD circuit according to the values of components $L_1$, $C_1$, $R_1$ and $R_2$ in Table 5. According to Equation (13), when the inductance decreases, the negative group delay increases. The cutoff frequency and the bandwidth increase. The simulation results are shown in Figure 6, from which the influence of inductance on the parameters of the low-pass negative group delay circuit can be seen.

**Table 5.** Data of low-pass negative group delay circuits with different $L_1$.

| State | $C_1$ (pF) | $L_1$ (nH) | $R_1$ (Ω) | $R_2$ (Ω) | $f_c$ (MHz) | $\tau(f_0)$ (ns) | IL (dB) |
|---|---|---|---|---|---|---|---|
| State1 | 0 | 470 | 50 | 50 | 9 | −3.13 | 3.52 |
| State2 | 0 | 200 | 50 | 50 | 22 | −1.33 | 3.52 |
| State3 | 0 | 100 | 50 | 50 | 44 | −0.67 | 3.52 |

$f_c$ represents the cutoff frequency when the group delay is zero. $\tau(f_0)$ represents the minimum negative group delay.

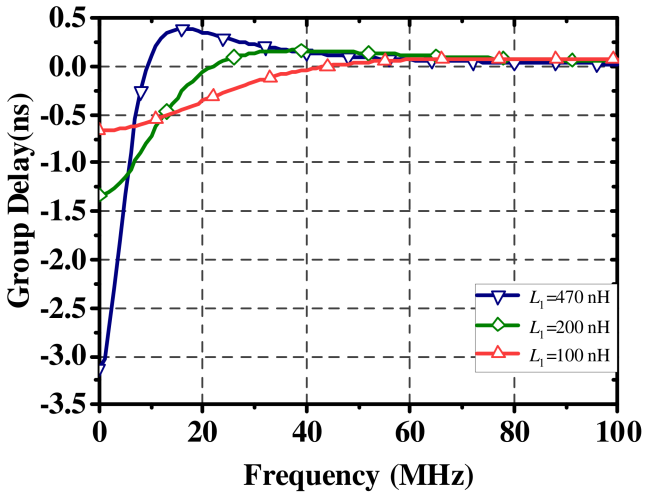


**Figure 6.** Group delay of low-pass negative group delay circuits with different capacitance.

## 4. Measurement and Discussion of NGD Circuit

### *4.1. Band-Pass Negative Group Delay Circuit*

When the element values are respectively $C_1$ = 1.6 pF, $L_1$ = 470 nH, $R_1 = R_2$ = 50 Ω, and $Z_0$ = 50 Ω, the group delay is $\tau$ = 8 ps > 0($f \approx 0$) and the frequencies are $f_2$ = 188.32 MHz, $f_1$ = 179.04 MHz and $f_0$ = 183.62 MHz under the condition of $\tau$ = 0. Calculation shows that $f_2 - f_0 \approx f_0 - f_1$. The conditions of forming a band-pass NGD circuit are satisfied. The circuit is fabricated according to the element values. This is shown in Figure 7a. The theoretical, simulated and measured waveforms of the negative group delay circuit are shown in Figure 7b. The insertion loss $S_{21}$ and reflection loss $S_{11}$ are shown in Figure 8. It can be seen from the theoretical waveform in the Figures 7b and 8 that all indicators are basically consistent with the results calculated by Equations (2) and (3). In the simulation, the Murata models of capacitors and inductors imported in ADS are used. These capacitor and inductor models include theoretical parameters and parasitic parameters. Due to the influence of parasitic parameters, the simulation results deviate from the theoretical calculation. The simulation results are different from the measured results in the minimum negative group delay and the center frequency corresponding to the minimum negative group delay, which is due to the influence of the actual element accuracy, PCB substrate and routing.

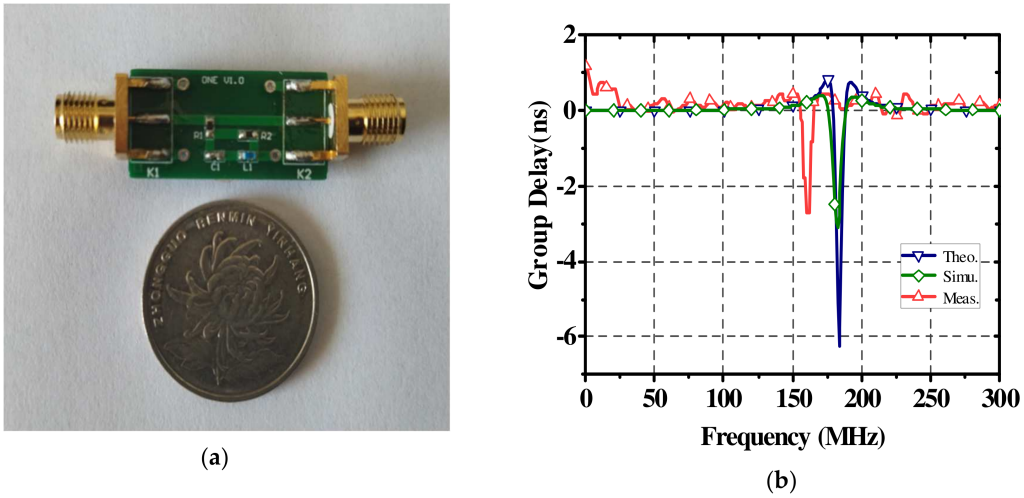


**Figure 7.** Band-pass NGD circuit (**a**) the fabricated band-pass NGD circuit; (**b**) negative group delay of band-pass NGD circuit.

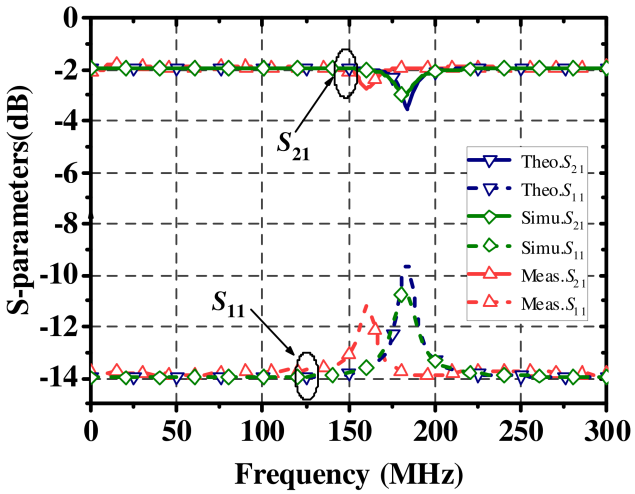


**Figure 8.** $S_{21}$ and $S_{11}$ of band-pass NGD circuit.

The comparison of the band-pass NGD with the reported literature is shown in Table 6. Compared with [18], the negative group delay is reduced by 4.26 ns, the bandwidth is increased by 8.78 MHz and the insertion loss is decreased by about 11.5 dB. Compared with paper [21], the negative group delay is reduced by 0.66 ns, and compared with paper [22], the negative group delay is reduced by 3.85 ns, and the insertion loss is decreased by 4.39 dB. It can be seen from the comparison that this design has better negative group delay and insertion loss.

**Table 6.** Performance comparison between band-pass negative group delay and reported NGD circuit.

| Literature | $f_0$ (MHz) | $\tau(f_0)$ (ns) | NGD Band (MHz) | IL (dB) |
|---|---|---|---|---|
| [18] | 1.5 | −1.8 | <0.5 | 15 |
| [21] | 97 | −5.4 | 20 | 3 |
| [22] | 22 | −2.21 | 89.91 | 7.9 |
| This work | 183.62 | −6.06 | 9.28 | 3.51 |

$f_0$ refers to the frequency at the minimum negative group delay. $\tau(f_0)$ (ns) refers to the minimum negative group delay.

### *4.2. High-Pass NGD Circuit*

When the element values are $C_1$ = 33 nF, $L_1$ = 3.9 nH and $R_1 = R_2 = Z_0$ = 50 Ω, the group delay is $\tau$ = 165 ns > 0($f \approx 0$), and the frequencies are $f_2$ = 1118.3 MHz, $f_1$ = 0.18 MHz and $f_0$ = 0.3 MHz under the condition of $\tau$ = 0, which meets the conditions for forming a high-pass negative group delay circuit. The fabricated high-pass NGD circuit is still shown in Figure 7a, except that the element values and the band-pass NGD circuit are different. The theoretical, simulation and measurement waveforms are shown in Figure 9a,b. It can be seen that the results of simulation and measurement are basically the same. Due to the limitations of the instrument, the measured data in Figure 9a,b are a straight line below 300 kHz.

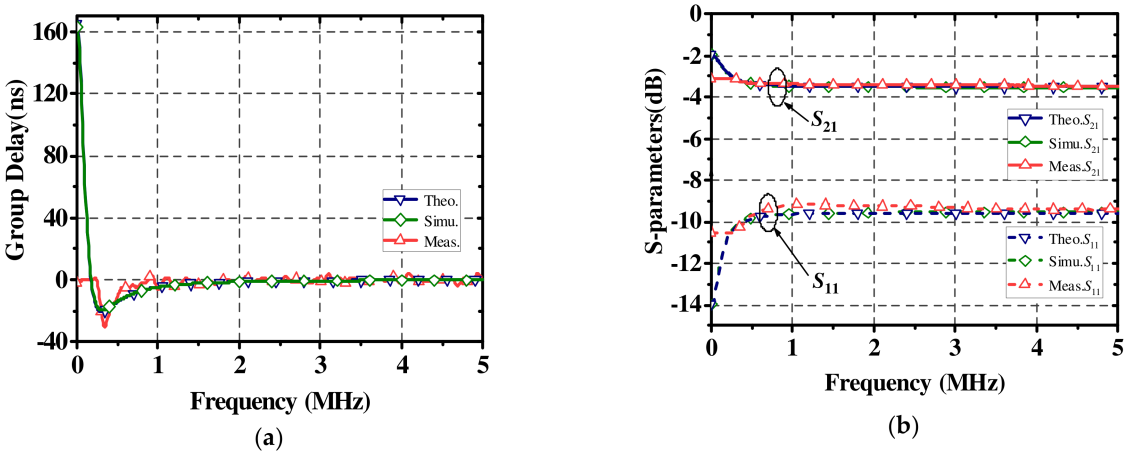


**Figure 9.** High-pass NGD circuit (**a**) group delay of high-pass NGD circuit. (**b**) $S_{21}$ and $S_{11}$ of high-pass NGD circuit.

There are few studies on high-pass negative group delay. In this paper, a negative group delay of −20.5 ns is realized in the low-frequency band, and the insertion loss is small. As the capacitance value increases, the negative group delay decreases, but it is limited to the test instrument and cannot render data. The performance comparison between the high-pass negative group delay circuit and the literature is shown in Table 7.

**Table 7.** Performance comparison between high-pass negative group delay and reported NGD circuit.

| Literature | $f_c$ (MHz) | $\tau(f_0)$ (ns) | IL (dB) | RL (dB) |
|---|---|---|---|---|
| [20] | 1 | −19.00 | / | / |
| [25] | / | / | 1.25~2.38 | <12 |
| This work | 0.176 | −20.50 | 1.96~3.51 | <9.56 |

$f_c$ refers to the frequency at the group delay $\tau$ = 0. $\tau(f_0)$ (ns) refers to the minimum negative group delay.

### *4.3. Low-Pass NGD Circuit Analysis*

The element values are $L_1$ = 470 nH and $R_1 = R_2 = Z_0$ = 50 Ω in the low-pass negative group delay circuit. Group delay is $\tau$ = −3.13 ns < 0($f$ = 0). The cut-off frequency is $f_c$ = 9.28 MHz when $\tau$ = 0, and the conditions of forming a low-pass negative group delay circuit are satisfied. The fabricated low-pass negative group delay circuit is shown in Figure 7a; only the element values are different from those of band-pass and high-pass.

The theoretical, simulation and measurement waveforms are shown in Figure 10a,b. It can be seen by comparison that these three results are basically the same.

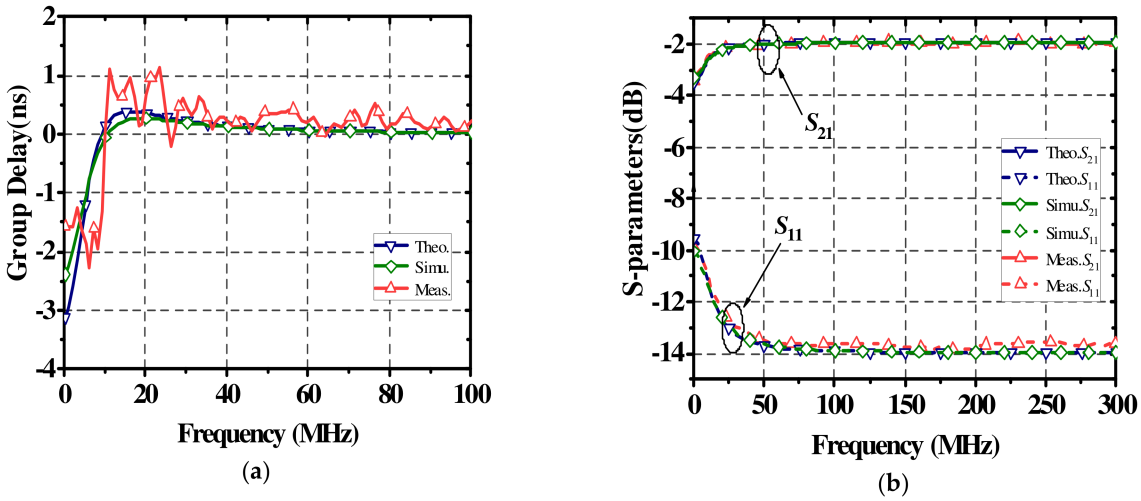


**Figure 10.** Theory, simulation and measurement of low-pass NGD circuits: (**a**) group delay; (**b**) $S_{21}$ and $S_{11}$.

Compared with the literature [19], although the negative group delay is larger, the insertion loss is increased by about 5.5 dB. This paper achieves a smaller negative group delay and insertion loss compared to [22]. The insertion loss at the minimum negative group delay is similar, but this paper achieves a smaller negative group delay, which is about 3 ns smaller than [24], as shown in Table 8. Considered comprehensively, the low-pass NGD circuit originally designed has good characteristics.

**Table 8.** Performance comparison between low-pass negative group delay and reported NGD circuit.

| Literature | $f_c$ (MHz) | $\tau(f_0)$ (ns) | NGD Band (MHz) | IL (dB) |
|---|---|---|---|---|
| [19] | 13.78 | −13.33 | <20 | 9 |
| [22] | 75.44 | −1.964 | 75.44 | 7.86 |
| [24] | 490 | −0.12 | 490 | 3.33 |
| This work | 9 | −3.13 | 9 | 3.52 |

## 5. Conclusions

The proposed multifunctional novel NGD circuit realizes the functions of band-pass, high-pass and low-pass negative group delay when the elements take different values, respectively. The circuit has good negative group delay characteristics, and the measured results are basically consistent with the theoretical design. Through calculation and simulation, the relationship between the elements and the negative delay circuit parameters is obtained. According to the authors' understanding, the existing NGD circuits all use one circuit to realize a single function. In this paper, three different NGD functions are realized with one circuit. These results provide a good theoretical basis for the flexible design and application of NGD circuits. In practical applications, the value of elements can be adjusted according to requirements, and various required negative group delay circuits can be obtained. This circuit is convenient to adjust, save costs and meet different application occasions. In the future, the NGD circuit can be used to realize the negative group delay of band-stop filters in the passband.

**Author Contributions:** Conceptualization, A.Y. and S.F.; methodology, A.Y. and Z.W.; software, A.Y. and H.L.; validation, A.Y.; formal analysis, A.Y. and Z.W.; investigation, A.Y. and H.L.; resources, S.F. and Z.W.; data curation, A.Y.; writing—original draft preparation, A.Y.; writing—review and editing, A.Y. and Z.W.; visualization, H.L.; supervision, S.F.; project administration, S.F.; funding acquisition, S.F. and Z.W. All authors have read and agreed to the published version of the manuscript.

**Funding:** This work was supported by the National Natural Science Foundation of China (Nos. 61871417 and 51809030), the Natural Science Foundation of Liaoning Province (Nos. 2019-MS-024

and 2020-MS-127), the Liaoning Revitalization Talents Program and the Fundamental Research Funds for the Central Universities (Nos. 3132021234 and 3132021231).

**Conflicts of Interest:** The authors declare no conflict of interest.

## References


1. Byun, G.S.; Navidi, M.M. A low-power 4-PAM transceiver using a dual-sampling technique for heterogeneous latency-sensitive network on-chip. *IEEE Trans. Circuits Syst. II Express Briefs* **2015**, *62*, 613–617. [CrossRef]
2. Esposito, D.; De Caro, D.; Napoli, E.; Petra, N.; Strollo, A.G. Variable latency speculative Han-Carlson adder. *IEEE Trans. Circuits Syst. I Regul. Pap.* **2015**, *62*, 1353–1361. [CrossRef]
3. Kim, K.J.; Di Renzo, M.; Liu, H.; Tsiftsis, T.A.; Orlik, P.V.; Poor, H.V. Distributed Cyclic Delay Diversity Systems with Spatially Distributed Interferers. *IEEE Trans. Wirel. Commun.* **2019**, *18*, 2066–2079. [CrossRef]
4. Lei, X.; Song, Y.; Yao, X.; Dong, B.; Jin, M. Effect of Group Delay on Channel Estimation Performance in OFDM System. *Appl. Math. Inf. Sci.* **2012**, *6*, 1037–1045.
5. Groenewold, G. Noise and group delay in active fifilters. *IEEE Trans. Circuits Syst. I Regul. Pap.* **2007**, *54*, 1471–1480. [CrossRef]
6. Huang, K.C.; Tung, S.L.; Juang, Y.T. Mean compensation based on projection-based group delay scheme for noisy speech recognition. *Electron. Lett.* **2002**, *35*, 1432–1434. [CrossRef]
7. Bartolini, M.; Pulici, P.; Stoppino, P.P.; Campardo, G. A reduced output ringing CMOS buffer. *IEEE Trans. Circuits Syst. II Express Briefs* **2007**, *54*, 102–106. [CrossRef]
8. Osaki, Y.; Hirose, T.; Matsumoto, K.; Kuroki, N.; Numa, M. Delay-compensation techniques for ultra-low-power subthreshold CMOS digital LSIs. In Proceedings of the 2009 52nd IEEE International Midwest Symposium on Circuits and Systems, Cancun, Mexico, 2–5 August 2009; pp. 503–506.
9. Liu, W.C.; Wei, T.C.; Huang, Y.S.; Chan, C.D.; Jou, S.J. All-digital synchronization for SC/OFDM mode of IEEE 802.15.3c and IEEE 802.11ad. *Trans. Circuits Syst. I Regul. Pap.* **2015**, *62*, 545–553. [CrossRef]
10. Gambuzza, L.V.; Buscarino, A.; Fortuna, L.; Frasca, M. Memristor-based adaptive coupling for consensus and synchronization. *Trans. Circuits Syst. I Regul. Pap.* **2015**, *62*, 1175–1184. [CrossRef]
11. Jabbour, C.; Fakhoury, H.; Loumeau, P. Delay-reduction technique for DWA algorithms. *IEEE Trans. Circuits Syst. II Express Briefs* **2014**, *61*, 733–737. [CrossRef]
12. Gupta, S.; Sounas, D.; Zhang, Q.; Caloz, C. All-pass dispersion synthesis using microwave C-sections. *Int. J. Circuit Theory Appl.* **2014**, *42*, 1228–1245. [CrossRef]
13. Ravelo, B. Neutralization of LC- and RC-Disturbances with Left-Handed and NGD Effects. *Adv. Electromagn.* **2013**, *2*, 73. [CrossRef]
14. Eudes, T.; Ravelo, B. Cancellation of delays in the high-rate interconnects with UWB NGD active cells. *Appl. Phys. Res.* **2011**, *3*, 81–88. [CrossRef]
15. Oh, S.S.; Shafai, L. Compensated circuit with characteristics of lossless double negative materials and its application to array antennas. *IET Microw. Antennas Propag.* **2007**, *1*, 29–38. [CrossRef]
16. Alomar, W.; Mortazawi, A. Method of generating negative group delay in phase arrays without using lossy circuits. In Proceedings of the 2013 IEEE International Wireless Symposium (IWS), Beijing, China, 13–18 August 2013.
17. Chaudhary, G.; Jeong, Y. A design of power divider with negative group delay characteristics. *IEEE Microw. Wirel. Compon. Lett.* **2015**, *25*, 394–396. [CrossRef]
18. Wan, F.; Wang, L.; Ji, Q.; Ravelo, B. Canonical Transfer Function of Band-Pass NGD Circuit. *IET Circuits Devices Syst.* **2019**, *13*, 125–130. [CrossRef]
19. Ravelo, B. First-order low-pass negative group delay passive topology. *Electron. Lett.* **2015**, *52*, 124–126. [CrossRef]
20. Ravelo, B. High-Pass Negative Group Delay RC-Network Impedance. *IEEE Trans. Circuits Syst. II Express Briefs* **2017**, *64*, 1052–1056. [CrossRef]
21. Ravelo, B.; Wan, F.; Nebhen, J.; Rahajandraibe, W.; Lalléchère, S. Resonance Effect Reduction with Bandpass Negative Group Delay Fully Passive Function. *IEEE Trans. Circuits Syst. II Express Briefs* **2021**. [CrossRef]
22. Ravelo, B.; Ngoho, S.; Fontgalland, G.; Rajaoarisoa, L.; Rahajandraibe, W.; Vauche, R.; Xu, Z.; Wan, F.; Ge, J.; Lallechere, S. Original Theory of NGD Low Pass-High Pass Composite Function for Designing Inductorless BP NGD Lumped Circuit. *IEEE Access* **2020**, *8*, 192951–192964. [CrossRef]
23. Ravelo, B.; Lalléchère, S.; Thakur, A.; Saini, A.; Thakur, P. Theory and circuit modeling of baseband and modulated signal delay compensations with low- and band-pass NGD effects. *AEUE Int. J. Electron. Commun.* **2016**, *70*, 1122–1127. [CrossRef]
24. Ravelo, B.; Wan, F.; Lallechere, S.; Rahajandraibe, W.; Thakur, P.; Thakur, A. Innovative Theory of Low-Pass NGD via-Hole-Ground Circuit. *IEEE Access* **2020**, *8*, 130172–130182. [CrossRef]
25. Ravelo, B. On the low-pass, high-pass, band-pass and stop-band NGD RF passive circuits. *Radio Sci. Bull.* **2017**, *363*, 10–27.
26. Choi, H.; Song, K.; Kim, C.D.; Jeong, Y. Synthesis of negative group delay time circuit. In Proceedings of the 2008 Asia-Pacific Microwave Conference, Hong Kong, China, 16–20 December 2008.
27. Choi, H.; Jeong, Y.; Lim, J.; Eom, S.; Jung, Y. A novel design for a dual-band negative group delay circuit. *IEEE Microw. Wirel. Compon. Lett.* **2011**, *21*, 19–21. [CrossRef]

28. Shao, T.; Wang, Z.; Fang, S.; Liu, H.; Chen, Z.N. A full-passband linear-phase band-pass filter equalized with negative group delay circuits. *IEEE Access* **2020**, *8*, 43336–43343. [CrossRef]
29. Qiu, L.F.; Wu, L.S.; Yin, W.Y.; Mao, J.F. Absorptive Bandstop Filter With Prescribed Negative Group Delay and Bandwidth. *IEEE Microw. Wirel. Compon. Lett.* **2017**, *27*, 639–641. [CrossRef]